Since January 2020 Elsevier has created a COVID-19 resource centre with free information in English and Mandarin on the novel coronavirus COVID-19. The COVID-19 resource centre is hosted on Elsevier Connect, the company's public news and information website.

International Journal of Biological Macromolecules 182 (2021) 1769–1784

Contents lists available at ScienceDirect

International Journal of Biological Macromolecules

journal homepage: http://www.elsevier.com/locate/ijbiomac

Ethyl cellulose coated sustained release aspirin spherules for treating COVID-19: DOE led rapid optimization using arbitrary interface; applicable for emergency situations

Sreejith Thrivikraman Nair [a,1], Kaladhar Kamalasanan [a,1,*], Ashna Moidu [a], Pooja Shyamsundar [a], Lakshmi J. Nair [a], Venkatesan P [b]

[a] Department of Pharmaceutics, Amrita School of Pharmacy, Amrita Institute of Medical Sciences and Research Centre, AIMS Health Sciences Campus, Amrita Vishwa Vidyapeetham, Kochi 682041, Kerala, India
[b] Department of Pharmacy, Annamalai University, Annamalainagar, Tamil Nadu, India

ARTICLE INFO

Article history:
Received 23 March 2021
Received in revised form 21 May 2021
Accepted 23 May 2021
Available online 26 May 2021

Keywords:
Sustained-release
Ethyl cellulose
Aspirin
Granules
Spheronization
Central composite design

ABSTRACT

This work attempts to resolve one of the key issues related to the design and development of sustained-release spherule of aspirin for oral formulations, tailored to treat COVID-19. For that, in the Design of Experiments (DOE) an arbitrary interface, "coating efficiency" (CE) is introduced and scaled the cumulative percentage coating (CPC) to get predictable control over drug release (DR). Subsequently, the granules containing ASP are converted to spherules and then to Ethyl cellulose (EC) Coated spherules (CS) by a novel bed coating during the rolling (BCDR) process. Among spherules, one with 0.35 mm than 0.71 mm shows required properties. The CS has a low 120^0 angle by Optical Microscopy (OM), smooth surface without cracks by scanning electron microscopy (SEM), and better flow properties (Angle of repose 29.69 ± 0.78^0, Carr's index $6.73 \pm 2.24\%$, Hausner's Ratio 1.07 ± 0.03) than granules and spherules. Once certain structure-dependent control over release is attained (EC coated spherules shows 10% reduction in burst release (BR) than uncoated spherules showing a release of 80–91%) the predictability is achieved and Design of space (DOS) by DOE (CE-70.14%and CPC-200% and DR-61.54%) is established. The results of DOE to experimentally validated results were within 20% deviation. The aspirin is changing its crystal structure by powder X-ray diffraction (PXRD) and differential scanning calorimetry (DSC) from Form-I to Form-II showing polymorphism inside the drug reservoir with respect to the process. This CE and CPC approach in DOE can be used for delivery system design of other labile drugs similar to aspirin in emergency situations.

1. Introduction

Cellulosic derivatives like ethyl cellulose (EC) [1], hydroxyl propyl methyl cellulose [2], and carboxy methyl cellulose [1,3] used alone or in combination with other macromolecules [1,4] are widely explored for drug delivery applications [5]. It is desirable to evaluate and analyze the role of these macromolecules in the design of the drug reservoir and rate-controlling membrane for producing the required delivery profile of the drug [6].

Various polymers from natural and synthetic origins are used for the said purpose. Ethyl cellulose is a semi synthetic hydrophobic polymer [7] that is currently being used as a sustained-release (SR) coating in various SR [8] and controlled release (CR) [9] formulations. Various EC-based value-added products are currently being developed [10–12]. The EC coating on solid dosage forms produces SR that helps in drug delivery for a long duration during the stay in the GIT [13]. EC coatings have better stability during storage, inertness, and good compressibility. On the other hand, the Eudragit L 100 (EL-100) is a synthetic anionic copolymer using for enteric-coated applications [14]. The site of drug delivery when using EL-100 is the jejunum and it dissolves at pH above 6 [15]. The use of EL-100 helps in site-specific drug delivery in the intestine [16]. On the other hand, EL-100 can be used as a polymer in combination with EC for modifying the release properties.

COVID-19 patients reported having cardiac complications [17], and WHO suggests anti-coagulants for the treatment [18]. Induction of coagulation cascade [19] seems to be the reason that can be suppressed using anticoagulants such as aspirin (ASP). Considering the fatality rate, rapidly translatable, affordable, and accessible anticoagulant technologies become significant in this scenario [20,21].

ASP has the triple effects of inhibiting virus replication, anticoagulant, and anti-inflammatory properties; now being tried for the

* Corresponding author.
E-mail address: kaladhar22654@aims.amrita.edu (K. Kamalasanan).
[1] Equal contributors

https://doi.org/10.1016/j.ijbiomac.2021.05.156
0141-8130/

prevention of COVID-19 related cardiac complications [22]. Recently, clinical trials have started to explore ASP as a protective agent to control cardiac complications in COVID-19 [23]. There are also reports that ASP has antiviral effects (100 mg/day), as it inhibits virus replication by inhibiting prostaglandin E2 (PGE2) in macrophages and up-regulation of type-1 interferon production [24]. Apart from that, a low dose (35–50 mg per day) of ASP is used as an anti-platelet agent for the prevention of cardiovascular events like stroke and myocardial infarction [23]. The antiplatelet effect (37.5 mg, 315 mg, 640 mg per day) is due to the inhibition of thromboxane A2 [25]. In this case, the solid dosage forms (SDF) such as ASP tablets or capsules75 mg (in an adult low-dose ASP) — to 325 mg (a regular strength tablet) need to be taken daily for a long time [26]. The daily intake of ASP by unmodified dosage forms leads to local side effects like mucosal irritation and ulceration in the gastrointestinal tract (GIT) due to the high concentration of ASP at absorption sites (70 to 140 mg/dL) [27]. Being an anionic drug ASP in the unionized form gets easily absorbed from the stomach [28]. On the other hand, ASP gets degraded to salicylate in stomach pH, thus, there is a requirement of reducing the degradation while improving the absorption and bioavailability.

For that the currently adopted strategy is to develop enteric-coated ASP- SDF to produce delayed-release that helps in reducing the acid degradation of the ASP molecule. On the other hand, enteric-coated systems completely avoid the possibilities of absorption in the stomach region, because the polymer completely avoids the release of the drug, as the polymer dissolves only at the intestinal pH [14,29]. In fact, it delivers the entire ASP in the intestine all of a sudden, where it is being least absorbed which causes local toxicity in a local concentration-dependent manner [21,27]. Also, enteric coating affects the anti-platelet activity of ASP due to low bioavailability [26,30].

These limitations can be overcome by the conversion of the enteric-coated to the SR solid dosage form [28] [31]. If ASP is delivered over a wide area using particulate carriers such as spherules in a sustained manner, it can substantially reduce the local concentration of the drug and can start the release from stomach and continue the release throughout the GI transit. Further, distributing the overall dose to a wide area has significance, as it enhances the mixing and release as well as the absorption from a wide area. So conversion of the unit solid dosage form as a spherule-based capsule can be a possible strategy [32]. These factors make the SR capsule more preferable than the delayed-release ASP tablet.

For developing the SR spherule formulation of ASP, the Physico-chemical aspects of the drug need to be analyzed for adopting suitable processing conditions. Earlier, poorly water-soluble drugs such as acyclovir (solubility 1.2–1.6 mg/ml) [33], ketoprofen (0.5 mg/ml) [34], and tamoxifen citrate (0.3 mg/l) [35] is explored for developing SR formulations. As compared to these drugs, ASP is further less soluble in water (2–4 μg/ml) [36] and is water-labile in nature [2]. The SR of water labile and poorly water-soluble drugs such as ASP is more challenging as the development of drug reservoirs requires special considerations [37,38].

Here, the wet granulation process is unavoidable for the preparation of granules, which is a prerequisite for preparing the spherules. In those conditions, ideally, keeping the solid state of the drug intact on a solid matrix helps to improve the chemical stability of the drug [39]. In such conditions, ASP-like labile drugs are blended with other ingredients and quickly transferred into a solid-state with a minimum amount of water required, as granules. This can be then sequentially layered with diluents to make spherules. This type of process improvement helps to ensure a minimum amount of water throughout the process of the formulation; from granules to coated spherules (CS) [40].

Spherules are being explored as a multi-particulate carrier for various SR drug delivery technologies. And they are being coated with rate-controlling polymer film coatings to produce SR spherules. For developing spherules, we have earlier developed a novel bed-coating-during-sliding (BCDS) process to prepare spherules from granules [2]. This can be converted into a “bed coating during rolling process” (BCDR) for coating the drug reservoir with the rate-controlling membrane. In this process during the conversion of granule to coated spherules, the intact control film coating is due to the rolling of the spherules, so the coating process needs to be considered as bed coating during rolling (BCDR). It's because spherules have a high chance of rolling than sliding (while in the case of granules, it slides due to its irregular shape). It can be adapted to any pharmaceutical operation such as pan coating [41] or Wurster process [42] for the commercial-scale production of spherules. Various SR polymer coatings using polymers such as EC and EL-100 are applied by Pan coating [43] and Wurster process [44] onto solid dosage forms [45,46].

Polymers with swellability, low water permeability (EC), or stimuli responsiveness (EL-100) are being generally used for developing the SR drug release coatings [47,48[49]]. For that, coating parameters need to be optimized [44], which is not well understood generally [50]. Subsequently, the coating performance can be thought of as an arbitrary criterion for assessing the effectiveness of a coating technique. For that, the “cumulative percentage coating” (CPC) and the “coating efficiency” (CE) can be introduced as independent variables that can influence the performance of the coating. These variables affect the responses such as overall control of drug release, drug content, and percentage size of spherules. This can be modeled in the Design of experiments (DOE) along with actual wet-lab experiments.

Design of experiments (DOE) by Quality by Design (QbD) is a statistical approach based on minimum available experimental data to systematically design further experiments [51]. The experimental design is done using appropriate statistical tools *in silico*. The process involves setting predefined objectives, parameterization of the components, and analyzing the set responses [52]. The major advantage of this technique is that multiple dependent and independent parameters are compared for their influence on the given responses to draw out the relations and interactions. The tools in QbD are, process analytical technology (PAT), risk assessment (RA), critical quality attributes (CQAs), and design of experiment (DOE) [51–53]. Among the various tools, DOE by central composite design (CCD) is used for optimizing formulation parameters to understand the Design of Space (DOS) in formulation development. Wherein, a set of dependent and independent formulation parameters and process variables are parameterized to analyze its interaction and relation to responses to get the boundary condition for a product with adequate quality, which can be later mathematically represented [52–54]. For identifying the DOS by DOE mainly Response Surface Methodology (RSM) is widely explored [55]. By employing DOE, this work aims to explore granules for the production of SR of ASP spherules and also to optimize the coating process. Regarding the control over the release of agents from the spherule, the coating of the rate-controlling membrane needs to be optimized. Here, CE and CPC are the two arbitrary independent variables that are parameterized and correlated to responses (drug content, drug release, and percentage size of spherules). In this work, CPC is equal to the amount of coating that produces a 10% decrease in drug release profile, which is taken as one number of the coating. Then it is multiplied by n number of coatings. This step-by-step approach helps to rationally achieve control over the release with respect to coating condition. So with a minimum set of experiments, the coating properties can be evaluated and optimized.

For that, the role of EC film coating properties in terms of CE on the SR of ASP spherules is predicted by DOE and tested experimentally. In addition, any polymorphic change in ASP needs to be understood and is studied using PXRD and DSC. This polymorphic change of ASP inside the drug reservoir is not well understood. This has significance in its solubility and release profile. ASP is shown to mainly exist in Form-I and under certain conditions is shifted to Form-II [56]. The study shows spherules can be successfully developed with excellent flow properties, high drug content, and SR properties by this method and the ASP inside the drug reservoir is showing polymorphism is first reporting here.

2. Materials and methods

2.1. Materials

ASP (180.15 g/mol), starch (359.3 g/mol), sodium lauryl sulfate (SLS) (288.3 g/mol), lactose (342.3 g/mol), hydrochloric acid, sodium hydroxide (0.1 N), potassium hydrogen orthophosphate, isopropyl alcohol, and acetone were purchased from Spectrum Reagents and Chemicals Pvt. Ltd., Kochi, India. Eudragit L-100 (1,25,000 g/mol), tartrazine dye (534.4 g/mol) were obtained from the Research-Lab Fine Chem Industries, Mumbai, India. Polyethylene glycol (62.07 g/mol) and ethyl cellulose (454.5 g/mol) were purchased from Loba Chemie Pvt. Ltd., Mumbai, India. Indigo dye (262.27 g/mol) was obtained from Sigma Aldrich chemicals Pvt. Ltd., Bangalore, India, and Talc (379.27 g/mol) from Vikash pharma, Mumbai, India. All the reagents are of AR grade.

2.2. Methods

2.2.1. Experimental design and response surface methodology (RSM)

In silico modeling and evaluation were performed and interpreted by Design Expert®12 Software (Stat-Ease, Inc.). The design selected here was the central composite design (CCD), and different formulation parameters such as CPC & CE were selected as independent variables. The drug release, drug content, and percentage size of spherules were considered as dependent variables. Percentage size of spherules here indicates the percentage spherule in a given bed of particles.

The selected variables and their levels are given in Table 1.

Analysis of Variance (ANOVA) was performed, and the *P*-value with a 95% confidence interval was evaluated in order to determine the significance of each coefficient term. And also to determine the fitting extent of experimental data, regression coefficient R^2 along with predicted and adjusted R^2 were determined. The equation for the current design:

$$Y = C + \beta 1A + \beta 2B + \beta 3AB + \beta 4A2 + \beta 5B2$$

where *Y* is the dependent variable,

C is the intercept and it is the arithmetic mean response of the 11 runs.

β1 to **β5** are the estimated coefficients for the corresponding factors A (CPC (%)) and B (CE(%)).

2.2.2. Scanning electron microscopy

Both the granules and spherules (coated and uncoated) were examined by scanning electron microscopy (SEM) (Phillips XL30) at 15–20 kV to study the surface morphology. Samples were mounted onto metal stubs using double-sided adhesive tape, vacuum-coated with gold (350 A°) in a Polaron E-5000, and analyzed by SEM.

2.2.3. Preparation of ASP granules [2]

ASP granules were prepared by wet granulation. The required quantity (Table 2) of ASP, lactose, starch, and SLS were taken in a mortar and pestle, and then triturated to form fine powders. The SLS was used as a wetting and wicking agent in the formulation. Starch paste (5% *w*/*v* starch powder in water) as a binding agent was added drop wise to form a coherent mass and it was made to pass through sieve no.12 (1.68 mm aperture size).

Table 1
Randomized response surface design parameters indicating the levels of variables.

Sl. no.	Independent variables	Coded	Low actual value	High actual value
1	Cumulative percentage coating (%)	X1	0	500
2	Coating efficiency (%)	X2	35	95

Table 2
Formula for the preparation of ASP granules.

Ingredients	Official quantity
ASP	300 mg
SLS	1 mg
Lactose	120 mg
Starch	24 mg
Starch paste	q.s

The starch solution was added during formulating spherules, in order to make it slightly sticky by making it wet, and excessive stickiness was avoided by adding the starch powder to the granules while coating [57].

2.2.4. Preparation of polymer-coated spherules by BCDR process

Wet granules were taken in a 250 ml beaker and were rotated at 45^0 angles clockwise (80–100 quarter rpm is converted to 20–25 rpm/min). To maintain the moisture of the granular bed, the ethanol: water (10:10 *v*/v) mixture was sprayed and the starch solution was added 6–7 drops (5 drops of 5% starch paste in 10 ml water).

Continuous rotation is done until the formation of spherical particles was observed. Dry granules are moistened before the coating process using the mixture of solvent ethanol: water (1:1 *v*/v), which helps in improving the coating without aggregation of the particles. Spherules were then coated using a suitable polymer ethyl cellulose (EC) or Eudragit L-100 (EL-100) coating solution by spraying using conventional bottle sprayers into a tilted (45°) glass beaker containing the spherule bed, and the spherules were then spread on a Petri dish for drying and kept at 60–70 °C (Normal drying temperature for the spherules) in a hot air oven for 20 min to prepare dried polymer-coated spherules [58]. In this work, four formulations with various SR coatings (based on ability to control the release rate) were prepared i.e., f1 (formulation 1), f2 (formulation 2), f3 (formulation 3), and f4 (formulation 4) respectively. Where, f1- is the uncoated spherules of ASP, f2- are spherules single coated with EC and EL-100 in 1:1 ratio, f3- is double-coated spherules, which was first coated with EC and then with EL-100, f4- are spherules double-coated with EC. Here isopropyl alcohol (IPA) and acetone were used as the solvents for preparing the coating solution for EC and EL-100 polymers (as shown in Table 3). While preparing EL-100 coating solution (5.99 g % *w*/*v* EL-100 in IPA 8.23 ml + Acetone 12.48 ml); In the case of EC (1.92 g % *w*/*v*) coating solution, 20.8 ml volume of acetone solution is applied to 10 g of spherules. The coating solution varies between each sample. The amount of coating solution utilized here is decided based on the quantity of coating solution required to produce a 10% control in the release. Wherein, this stepwise approach helps to rationally achieve control over the release with respect to coating conditions. After coating with sustained-release polymers, they are sieved and separated to sieve no. 22 (aperture size - 0.71 mm) and 44 (0.35 mm) size spherules.

Table 3
Formulae for preparation of coating solution of ethyl cellulose and eudragit L-100.

Ingredients	Coating solution for 10 g of spherules	
	Ethyl cellulose	Eudragit L-100
Ethyl cellulose	0.416 g	–
Eudragit L-100	–	1.24 g
Talc	0.33 g	–
PEG	–	0.2 g
Isopropyl alcohol	–	8.23 ml
Acetone	20.8 ml	12.48 ml
Dye	0.08 g	0.08 g

2.2.5. Microscopic evaluation of granules and spherules

A projection microscope was used to determine the shape and surface properties of granules and spherules. The prepared granules and spherules were taken in a glass slide and were observed through a projection microscope (10×). The shape and edges of the particles were studied and the edges at 45^0, 90^0, 120^0 were counted and the percentage edges were calculated.

2.2.6. Flow property studies

The parameters such as Angle of repose, Carr's index, Hausner's ratio of spherules (retained in sieve no.22, and 44 of each coating) were calculated.

2.2.6.1. Angle of repose [59]. It determines the maximum angle between the cone of the pile of spherules and the horizontal plane. Spherules were taken in the funnel and were made to fall freely on paper to form a pile. The radius and height of the pile were measured.

$$\text{Angle of repose } (\tan\theta) = h/r$$

where 'h' is the height and 'r' is the radius of the pile.

2.2.6.2. Particle packing parameters [2]. For measuring bulk density, spherules (20 g) were taken in a 100 ml measuring cylinder and the initial volume was noted. It was then tapped to determine the final volume occupied.

$$\text{Bulk density} = \text{Spherule weight}/\text{Bulk volume}$$

For measuring tapped density, spherules (20 g) were taken in a 100 ml measuring cylinder and the initial volume was noted. It was attached to a tapped density apparatus and the final volume occupied after 100 tappings were noted.

$$\text{Tapped density} = \text{Spherule weight}/\text{Tapped volume}$$

The Carr's index or Carr's compressibility Index indicated the compressibility of powder or granule, thus, an indicator of interstitial space between the particles upon confinement. That in turn reflected the shape of the particles. For spherical particles, like spherules, the interstitial space remained low, thus, Carr's index was high, while for granular particles having an irregular shape, the interstitial space was high, so, the flow property and compressibility were low [2].

$$\text{Carr's index} = [\text{Tapped density} - \text{Bulk density}/\text{Tapped density}] \times 100$$

Hausner's ratio was determined using the ratio between the tapped and bulk density.

$$\text{Hausner's ratio} = \text{Tapped density}/\text{Bulk density}$$

2.2.7. Drug content evaluation [60]

ASP spherules (50 mg) were accurately weighed, triturated and dissolved in a phosphate buffer of pH 6.8, and filtered. Absorbance was taken at λ_{max} 275 nm by using a UV/Vis spectrophotometer by keeping phosphate buffer as blank [61].

2.2.8. Drug release studies [62]

Percentage drug release with respect to time was determined using USP type 1 basket apparatus. Phosphate buffer (900 ml) of pH 6.8 was taken and 1.5 g of spherules were added to it. To maintain the sink condition, the apparatus was rotated at 75 rpm at 37 ± 0.5 °C temperature. As the Steady-state flow of release medium in USP type 1 basket apparatus, rotating at the speed above 50 rpm ensures steady state sink condition [63]. Moreover, to analyze the mechanism of release from less intact rate-controlling films coated over the drug reservoir spherules, turbulence during mixing should not be an error contributing factor, so a reasonable 75 rpm was selected based on the total amount of drug released from uncoated spherules. Subsequently, this mixing was good enough to maintain steady-state diffusion of the drug molecule during dissolution.

At various intervals, 1 ml of release medium was withdrawn (1, 2, 3, 4, 5, and 6 h.) and the same amount of buffer was replaced. Absorbance was taken at 275 nm using a UV- Vis spectrophotometer.

2.2.9. Kinetic modeling [69,70]

The kinetics and mechanism of drug release from spherules were determined by fitting the in-vitro drug release data into Zero order, First order, Higuchi, and Korsmeyer-Peppas model. The best-fitted model was confirmed using R^2 and n values.

2.2.9.1. Zero-order release. It showed the release of the drug at a constant rate. To acquire the data a graph was plotted between cumulative percentage drug released against time:

$$Q_t = Q_0 + K_0 t$$

where Q_t = Drug released in time 't'.
Q_0 = Initial drug content.
K_o = Rate constant of zero-order release.

2.2.9.2. First-order release. The release depended on the concentration. To acquire the data a graph was plotted between log cumulative percentage drug remaining against time.

$$\text{Log}Q_t = \text{Log}\, Q_0 - K_t/2.303$$

where Q_t = Drug released in time 't'.
Q_0 = Initial drug content.
K_t = Rate constant of the first-order release.

2.2.9.3. Higuchi model. To acquire the data, a graph was plotted between cumulative percentage drug release against the square root of time.

$$Q_t = K_H\, t^{1/2}$$

where Q_t = Amount of drug release at the time "t".
K_H = Higuchi release rate constant.

2.2.9.4. Korsmeyer–Peppas model. After acquiring the data, a graph was plotted between log cumulative percentage drug release v/s log time.

$$Q_t/Q_0 = K_{kp}\, t^n$$

where, Q_t/Q_0 = Fraction of drug release at time 't'.
K_{kp} = Korsmeyer-Peppas release rate constant.
n = Diffusion constant.

2.2.10. Powder X-ray diffraction (PXRD) analysis

The PXRD measurements were done using a Bruker AXS D8 Advance x-ray diffractometer. All samples were investigated in a polycrystalline form. Each sample was powdered in an agate mortar and the x-ray measurements were carried out at room temperature (25 °C), Step Size = 0.020°, 2θ =3°-70° and Wavelength = 1.54060 Å.

2.2.11. Differential scanning calorimetry (DSC) analysis

The DSC studies were done using a NETZSCH DSC 204F1 Phoenix. The DSC measurements were carried out in the flowing air atmosphere (N_2, 40. 0 ml/min/N_2, 60.0 ml/min) with a heating rate of 20 °C/10.0(K/min) at 20–200 °C.

Table 4
Design model indicating the levels of variables and responses.

Run	Cumulative percentage coating (CPC) (%)	Coating efficiency (CE) (%)	Drug release (%)	Percentage size of spherules (%)	Drug content (%)
1	300	65	41.66	52.04	53.1
2	300	95	49	69.11	65.4
3	150	65	63.01	67.22	57.01
4	150	65	46.3	83.5	53.01
5	150	35	59.4	79.62	49.25
6	0	65	58.02	83.01	55.74
7	300	35	39.01	52.36	52.1
8	150	65	53.68	69.74	49.65
9	0	35	79.89	85.54	50.7
10	150	95	59.4	74.2	66.2
11	0	95	67.5	82.9	65.4

2.3. Statistical analysis

The experimental data were analyzed statistically and represented as Mean ± S.D. All the data represented were done with a minimum three number of samples; wherever more samples are done it was mentioned specifically. The microscopic images are done using representative samples.

3. Result and discussion

3.1. Experimental design

In this work, a randomized response surface design experiment is conducted for the SR of polymer-coated ASP spherules in order to assess the influence of two different independent variables (CPC and CE) on the responses such as drug content, drug release, and the percentage size of spherules. The different interactions and multiple effects between each parameter are verified and studied using Design-Expert software (v.12). The experimental trials are performed at all 11 possible combinations according to the model and the results are shown in Table 4 and Fig. 1.

Fig. 1 shows the role of independent variables such as CE and CPC on drug release. Fig. 1(a) shows the ANOVA results for the optimization of drug release, for that, the statistical data of dependent variables (drug release (DR), drug content (DC), percentage size of spherule (PS)) obtained are introduced to ANOVA and are found to be significant at $p < 0.05$. That indicates in this case, A (CPC) is the significant model term. The overall interactions were found to be significant at $p < 0.05$, which shows the effect of both variables in combination, is also significant on the mean drug release. The Lack of fit value for $p > 0.05$ indicates, the noise of the experiments is non-significant. Fig. 1(b) shows

(a)

Source	Sum of Squares	Df	Mean Square	F-value	p-value	
Model	1212.26	5	242.45	5.78	0.0384	significant
A. Cumulative percentage coating	956.09	1	956.09	22.79	0.005	
B-coating efficency	0.96	1	0.96	0.0229	0.8857	
AB	125.22	1	125.22	2.98	0.1446	
A^2	14.79	1	14.79	0.3526	0.5785	
B^2	129.28	1	129.28	3.08	0.1395	
Residual	209.76	5	41.95			
Lack of Fit	69.51	3	23.17	0.3304	0.8092	not significant
Pure Error	140.25	2	70.12			
Cor Total	1422.02	10				

(b)

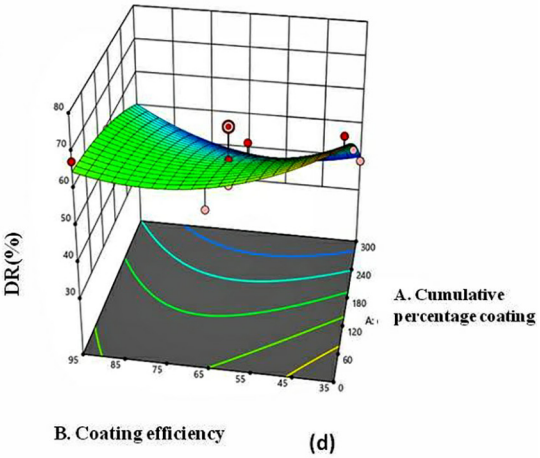

(c)

Factor	Coefficient Estimate	df	Standard Error	95% CI Low	95% CI High	VIF
Intercept	53.5	1	3.32	44.96	62.04	
A. Cumulative percentage coating	-12.62	1	2.64	-19.42	-5.83	1
B. Coating efficiency	-0.4	1	2.64	-7.2	6.4	1
AB	5.59	1	3.24	-2.73	13.92	1
A^2	-2.42	1	4.07	-12.88	8.04	1.08
B^2	7.14	1	4.07	-3.32	17.6	1.08

(d)

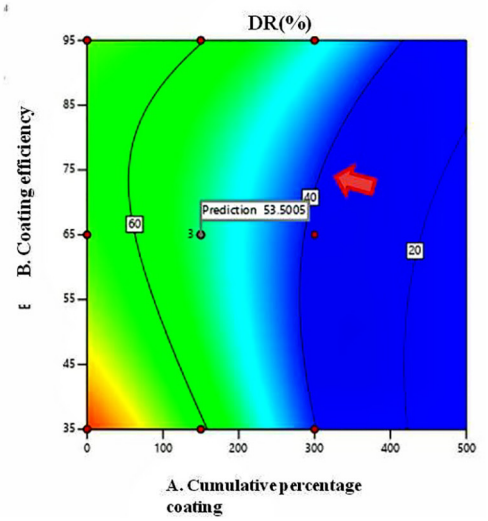

Fig. 1. Effect of independent variables such as CE and CPC on drug release (DR), (a) ANOVA responses for the drug release of ASP granules. (b) Response 3D plot of independent variables up on drug release, (c) Coefficient of estimate values for drug release of ASP granules, (d) Contour plot for the effect of CPC, and CE on drug release.

the graphical interpretation of interaction using a 3-D plot, which is highly recommended and is used to assess the interactive effect of the process variables and the predictability. Fig. 1(c) shows the coefficient of estimate values for drug release, which indicates that all values are negative for the main effects and interactive effects. The main effects of A and B as well as interaction terms (AB, A^2, and B^2) show how the responses change when 2 variables are simultaneously changed. This in turn shows all the independent variables (CE and CPC) have a favorable effect on a decrease in the release of drugs from spherules and are predictable. Fig. 1(d) shows the contour plot of drug release in 2-D, with A & B (independent variables), plotted on X and Y scales and response values represented by contours (*Z*-scale). These plots are useful for establishing the response values and operating conditions as required. The figure shows as the CE (>60%) and CPC (>200%) increases; the drug release below 60% can be attained and is predictable.

Fig. 2 shows the role of independent variables such as CE and CPC on the percentage size of spherules. Fig. 2(a) shows the ANOVA results for the optimization of the percentage size of spherules (PS), which are found to be significant at $p < 0.05$. In this case, A (CPC) is the significant model term. The overall interactions were found to be significant at $p < 0.05$, which shows the effect of both variables in combination is also significant on the mean percentage size of spherule. The Lack of fit value for $p > 0.05$ indicates, the noise of the experiments is non-significant. Fig. 2(b), shows the graphical interpretation of the percentage size of spherule (PS) using a 3-D plot, which is highly recommended and is used to assess the interactive effect of the process variables and the predictability. Fig. 2(c) shows the coefficient of estimate values for the percentage size of spherule (PS), which indicates that the values (AB, B^2 and B) are positive for the main effects and interactive effects. This in turn shows all the independent variables (CE and CPC) have a favorable effect on an increase in the percentage size of spherule and are predictable. Fig. 2(d) shows the contour plot of percentage size of spherule (PS) in 2-D, with A & B (as independent variables), plotted on X and Y scales and response (PS) values represented by contours (*Z*-scale). The figure shows as the CE (>60%) and CPC (>200%) increases, there is a favorable effect on an increase in the percentage size of spherule, which in turn controls the release profile.

Fig. 3 shows the role of independent variables such as CE and CPC on the drug content. Fig. 3(a) shows the ANOVA results for the optimization of drug content (DC), which are found to be significant at $p < 0.05$. The overall interactions were found to be significant at $p < 0.05$, which shows the effect of both variables in combination, is also significant on the mean drug content. The Lack of fit value for $p > 0.05$ indicates, the noise of the experiments is non-significant.

Fig. 3(d) and 3(b) shows the contour plot and 3-D response plot for drug content (DC) in 2-dimensional and 3-dimensional plane, with A &

(a)

Source	Sum of Squares	df	Mean Square	F-value	p-value	
Model	1208.59	5	241.72	5.36	0.0446	significant
A-cumulative percentage coating	1012.44	1	1012.44	22.44	0.0052	
B-coating efficency	12.59	1	12.59	0.2789	0.62	
AB	93.99	1	93.99	2.08	0.2085	
A^2	67.37	1	67.37	1.49	0.2762	
B^2	45.29	1	45.29	1	0.3624	
Residual	225.6	5	45.12			
Lack of Fit	72.03	3	24.01	0.3127	0.8196	not significant
Pure Error	153.58	2	76.79			
Car Total	1434.19	10				

(b)

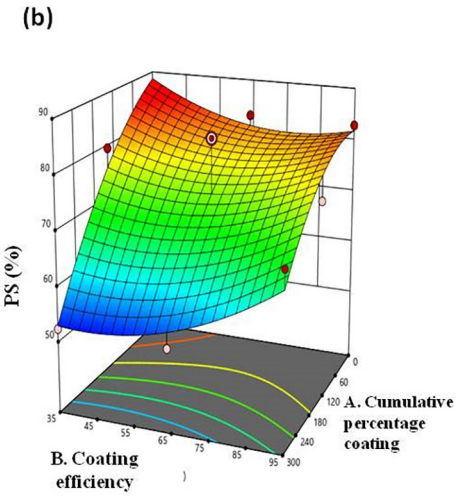

(c)

Factor	Coefficient Estimate	df	Standard Error	95% CI Low	95% CI High	VIF
Intercept	73.16	1	3.45	64.31	82.02	
A-cumulative percentage coating	-12.99	1	2.74	-20.04	-5.94	1
B-coating efficency	1.45	1	2.74	-5.6	8.5	1
AB	4.85	1	3.36	-3.79	13.48	1
A^2	-5.16	1	4.22	-16.01	5.69	1.08
B^2	4.23	1	4.22	-6.62	15.08	1.08

(d)

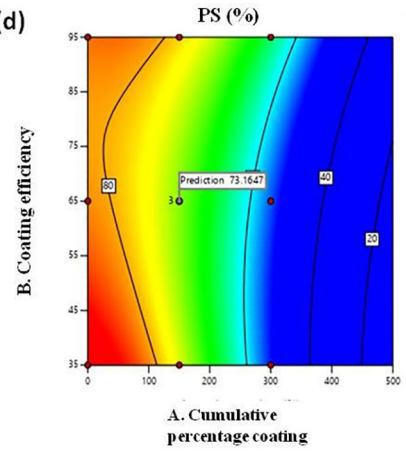

Fig. 2. Effect of independent variables such as CE and CPC on percentage size of spherules, (a) ANOVA responses for the percentage size of spherules, (b) Response 3D plot of independent variables upon percentage size of spherules, (c) Coefficient of estimate values for percentage size of spherules, (d) Contour plot for the effect of CPC, and CE on percentage size of spherules for ASP granules.>.

(a)

Source	Sum of Squares	df	Mean Square	F-value	p-value	
Model	394.22	5	78.84	11.61	0.0088	significant
A. Cumulative percentage coating	:563	1	0.2563	0.0377	0.8536	
B-coating efficency	336.75	1	336.75	49.6	0.0009	
AB	0.49	1	0.49	0.0722	0.7989	
A^2	2.15	1	2.15	0.3173	0.5976	
B^2	45.27	1	45.27	6.67	0.0493	
Residual	33.94	5	6.79			
Lack of Fit	6.79	3	2.26	0.1667	0.9105	not significant
Pure Error	27.15	2	13.58			
Cor Total	428.16	10				

(b)

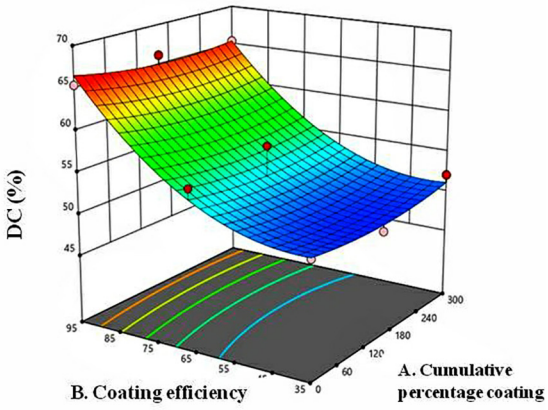

(c)

Factor	Coefficient Estimate	df	Standard Error	95% CI Low	95% CI High	VIF
Intercept	53.33	1	1.34	49.9	56.77	
A. Cumulative percentage coating	-0.2067	1	1.06	-2.94	2.53	1
B-coating efficency	7.49	1	1.06	4.76	10.23	1
AB	-0.35	1	1.3	-3.7	3	1
A^2	0.9221	1	1.64	-3.29	5.13	1.08
B^2	4.23	1	1.64	0.019	8.44	1.08

(d)

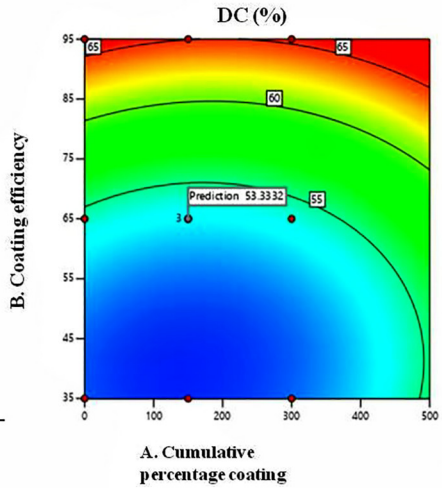

Fig. 3. Effect of independent variables such as CE and CPC on drug content. (a) ANOVA responses for the drug content of ASP spherules. (b) Response 3D plot of independent variables up on drug content of spherules. (c) Coefficient of estimate values for drug content of spherules. (d) Contour plot for the effect of CPC, and CE on the drug content of ASP spherules.

B (as independent variables), plotted on X and Y scales and response (DC) values represented by *Z*-scale. The figure shows as the CE (>60%) and CPC (>200%) decrease in the drug content below 70% can be attained and is predictable.

Fig. 3(c) shows the coefficient of estimate values for drug content (DC), which indicates all the coefficient estimates except model terms (A^2, B^2, and B) are negative, for the main effects and interactive effects. This is in turn shows all the independent variables (CE and CPC) have a favorable effect on a decrease in drug content of spherules.

The coefficient estimate represents the expected change in response per unit change in factor value when all remaining factors are held constant. The intercept in an orthogonal design is the overall average response of all the runs. The coefficients are adjustments around the average based on the factor settings. When the factors are orthogonal the VIFs (Variance inflation factor) are 1; VIFs greater than 1 indicate multi-collinearity, the higher the VIF better the correlation of factors. As a rough rule, VIFs less than 10 are tolerable [66]. In this model, the variance of inflation factor is found to be 1, which indicates there is no multi-collinearity among the factors and also verifies that it is in good agreement to proceed with regression. The regression analysis of variance for these dependent variables is given in Table 5.

The correlation coefficient for the models is also calculated, which are found to be >0.8 indicating a strong fit. The predicted R^2 for these dependent variables is found to be in reasonable agreement with the adjusted R^2 i.e. the difference is less than 0.2. The adequate precision here measures the signal-to-noise ratio. A ratio greater than 4 is desirable [67]. Here, ratios for the model indicate an adequate signal and verify that this model can be used to navigate the design space.

3.2. Optimized ASP spherules

The variables used in obtaining ASP spherules played a major role in determining the coating requirements for the desired control over

Table 5
Regression analysis of the following dependent variables.

Response	Drug release	Percentage size of spherules	Drug content
R^2	0.8525	0.9207	0.8427
Adjusted R^2	0.705	0.8414	0.6854
Predicted R^2	0.6266	0.7165	0.7741
Adeq Precision	8.0244	8.5548	7.1911

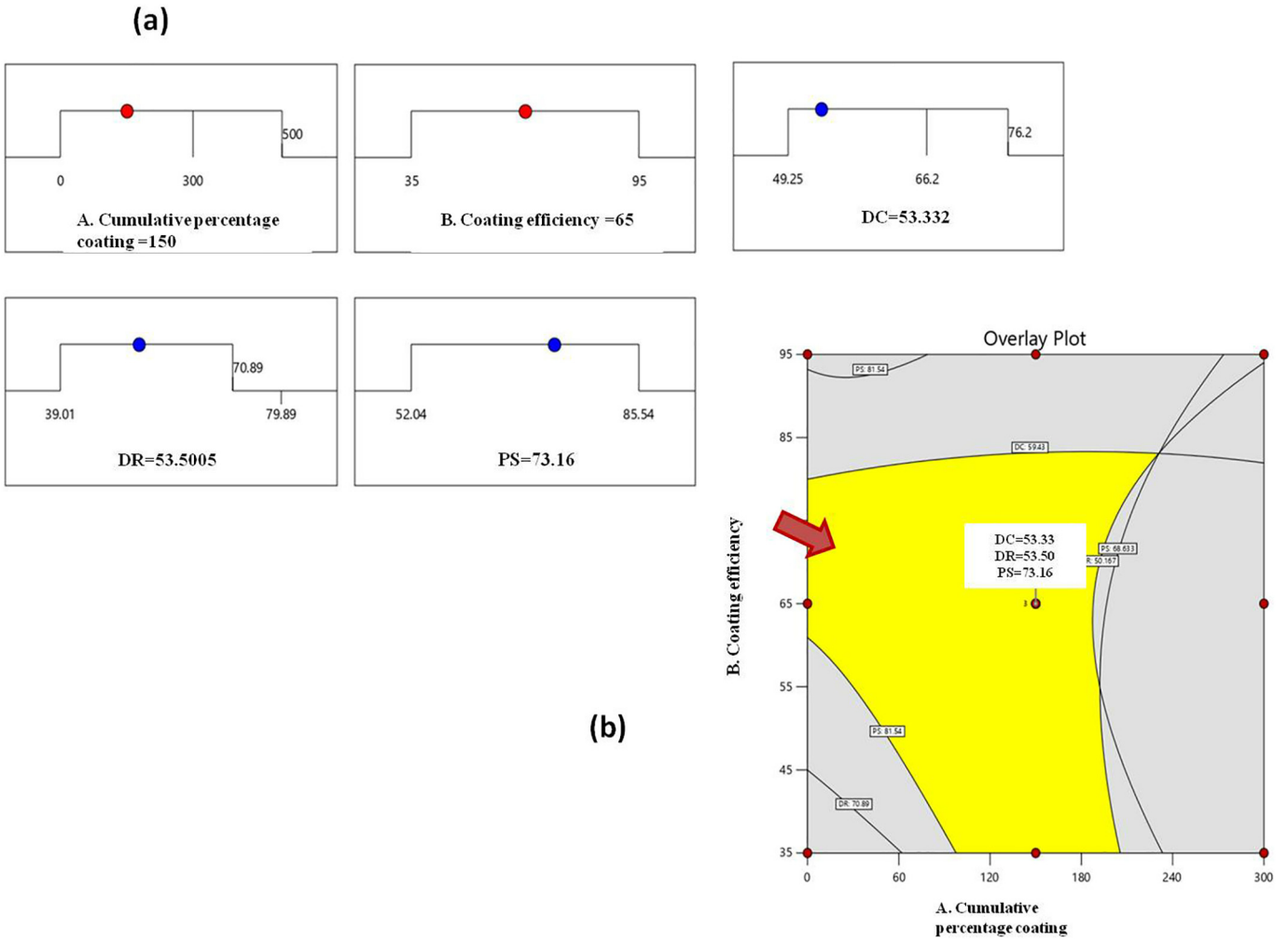

Fig. 4. DOS of optimized spherules, (a) Numerical optimization ramp view for CE, CPC, drug release (DR), drug content (DC), and percentage size of spherules (PS). (b) Shows the Design of Space (DOS) on contour plot for optimized levels of independent variables for the DC, DR, and PS.

release along with other properties. ASP spherules with proper uniform coating and maximum CE are desired to achieve the slow release of the drug over a wide area.

The optimization study of these experimental results is performed by keeping all responses within desired ranges by using response surface methodology. In this case, CE is targeted to the maximum and other variables are kept in range for achieving the desired effect. Based on the recommended values as given in Fig. 4, the experiment is conducted to validate the optimized results. According to the results obtained, approximately by a CPC of 200% or two coatings, 70.14% of maximum CE is achieved with a slow release of ASP with maximum release up to 61.54% in the given time. This indicates a reasonable agreement of the experimental and predicted results under optimized conditions as shown in Table 6. Also, based on these results, it can be concluded that the statistical data obtained from the experimental design are quite helpful in understanding the interactions and main relations of the independent variable. Also, helps to formulate the desired formulation at suitable conditions with reproducibility for an optimum coating process.

Fig. 4(a) shows the optimized ramp view of numerical values for CE, CPC, drug release, drug content, and percentage size of spherules in the ramp plot. The colored dot on each ramp shows the factor setting or response prediction for that solution. Wherein, Fig. 4(b) the colored region with an arrow showing the design of space for CE, CPC, drug release, drug content, and percentage size of spherules in a contour plot with optimized values. This overlay plot helps to visually identify an area where the predicted means of one or more response variables are in an acceptable range.

The optimized granules are prepared by the wet granulation method followed by converting granule to spherule by BCDR process (Fig. 5). This helps in reducing the degradation of ASP during the process. As during the process; ASP in the solid form is maintained throughout the inside of the granule, and is minimally exposed to the water from the starch paste, which is applied during starch coating to prepare spherules from granules. This step increases the stability of labile hydrolysable drugs like ASP than conventional wet granulation process [68,69]. The solid-state stability of ASP is relatively high even in a hygroscopic environment [70]. The aqueous starch is used here for the spheronization process [71] to convert granules to spherules.

Table 6
Optimized values for corresponding predicted and actual factors and variables.

Variables	Predicted	Actual	Desirable
Cumulative percentage coating (CPC) (%)	150	200	100–250
Coating efficiency (CE) (%)	65	70.14	55–90
Drug release (%)	53.50	61.54	45–70
Drug content (%)	53.32	71.55	50–85
Percentage size of spherules (%)	73.16	70	60–80

[a]

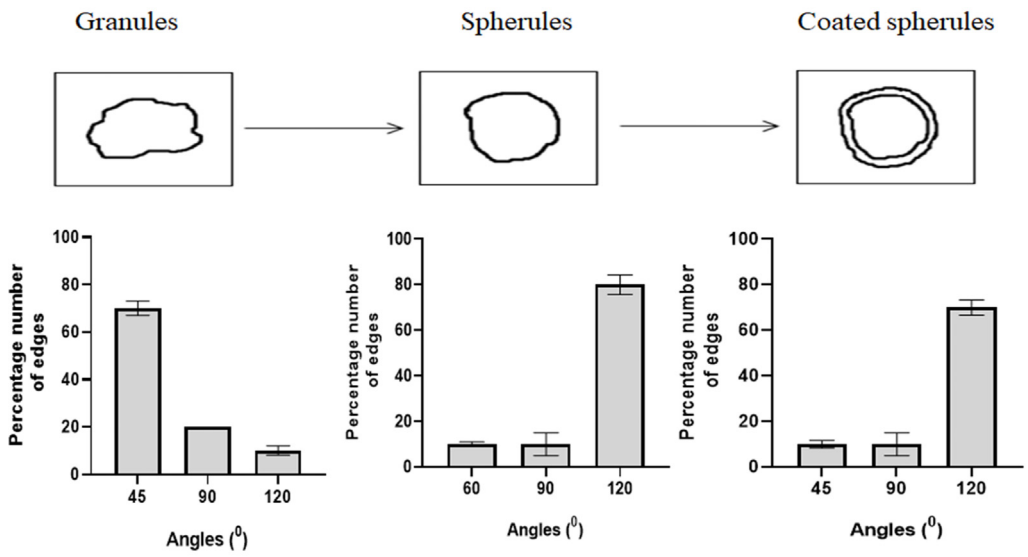

[b]

Spherules	Angle of repose (0)	Bulk density (g/ml)	Tapped density (g/ml)	Carr's index (%)	Hausner's ratio	Flow property
US-22	32.11±0.1	0.64±0.01	0.674±0.01	5.303±1.80	1.056±0.02	Excellent
US-44	26.37±0.32	0.631±0.01	0.697±0.01	9.473±0.17	1.104±0.002	Excellent
S-EC-EG-C1-22	27.22±0.57	0.577±0.01	0.612±0.01	5.762±0.108	1.061±0.001	Excellent
S-EC-EG-C1-44	25.46±0.53	0.55±0.01	0.58±0.01	5.542±0.18	1.06±0.001	Excellent
S-EC-EG-C2-22	29.10±0.91	0.472±0.01	0.51±0.01	7.09±2.25	1.08±0.02	Excellent
S-EC-EG-C2-44	29.69±0.78	0.461±0.01	0.49±0.01	6.733±2.24	1.07±0.03	Excellent

Fig. 5. Comparison of granules, spherules and coated spherules. (a) Morphological comparison between granules, spherules, and coated spherules. (b) Flow property studies like the angle of repose, bulk and tapped density, Carr's index, and Hausner's ratio of corresponding coated and uncoated spherules.

Subsequently, to reduce the influence of water a mixture of non – aqueous solvent (ethanol) with water is used to reduce the drying time. Since ethanol reduces the water surface tension, the evaporation rate of water is increased; in addition, the hydrolysable nature of water is reduced. That also helps in increasing the stability of ASP.

The spherules are then coated with a suitable sustained release polymer coating to control the release [72]. That is sieved to obtain two different ranges of spherules and classified as one retained in sieve no.22 (aperture size −0.71 mm.) and others in sieve no.44 (aperture size 0.35 mm).

In the case of coated spherules; EC exhibits good film properties and the compact film is often required for better control over release. EC film shows tackiness thus; an anti-tacking agent such as talc is added. EL-100 with PEG is not showing much tackiness and talc is not required. While EL-100 film requires a porous structure as per our studies subsequently the PEG is added.

Subsequently, the granules, spherules, and coated spherules are studied in detail for their morphology (optical microscopy and SEM), flow properties, drug content, and drug release properties.

At first, the particles (granules, spherules, and coated spherules) are studied by optical microscopy (Fig. 5). The surface edges and the percentage number of angles are studied and calculated to differentiate the granules from spherules. The acute (45^0) or right (90^0) angle edges are more in granules (approx. 70%), while the spherules have more obtuse (120^0) angles (approx. 80%) due to their smooth surfaces as shown in Fig. 5.

Flow property studies like the angle of repose, bulk and tapped density, Carr's index, and Hausner's ratio of the uncoated spherules (US-22/44); single coated EC and EL-100 spherules (S-EC-EG-C1-22/44); double-coated EC and EL-100 (S-EC-EG-C2-22/44); double-coated EC spherules (S-EC-C2-22/44) are found to be excellent as shown in Fig. 5.

During the coating process, the particles in the bed need to be properly rolled down, for optimum coating around the particles. Spherical particles have better flow properties than granular particles, thus the efficiency of coating on spherical particles is high. These results are comparable with a previous report of the formulation of different polymer-coated spherules from granules [2].

3.3. Scanning electron microscopy

The SEM studies show the information about the microscopic features regarding surface morphology, shape, and size of the particles as well as characteristics of the film coating [73]. In the case of granules (Fig. 6a) shows the particle with irregular shape and edges along with cracks. While that of spherules appeared (Fig. 6b) regular sphere with cracks. While the coated spherules (Fig. 6c) show a regular sphere shape with reduced cracks. The size of both spherules is greater than granules. Further, the surface topography is analyzed at higher magnification. The granules (Fig. 6d–f) show regularly distributed packed particles at the surface of granules, spherules, and coated spherules. The interstitial space between the particles at the surface of granules, spherules, and coated spherules (Fig. 6g–i) appeared the same. While that on the surface of coated spherules have shown deposited polymeric material between the particles (Fig. 6i). From the SEM studies, it is apparent that the shape of the particles is becoming spherical in the case of spherules, the intra-particular cracks are getting reduced after the EC coating

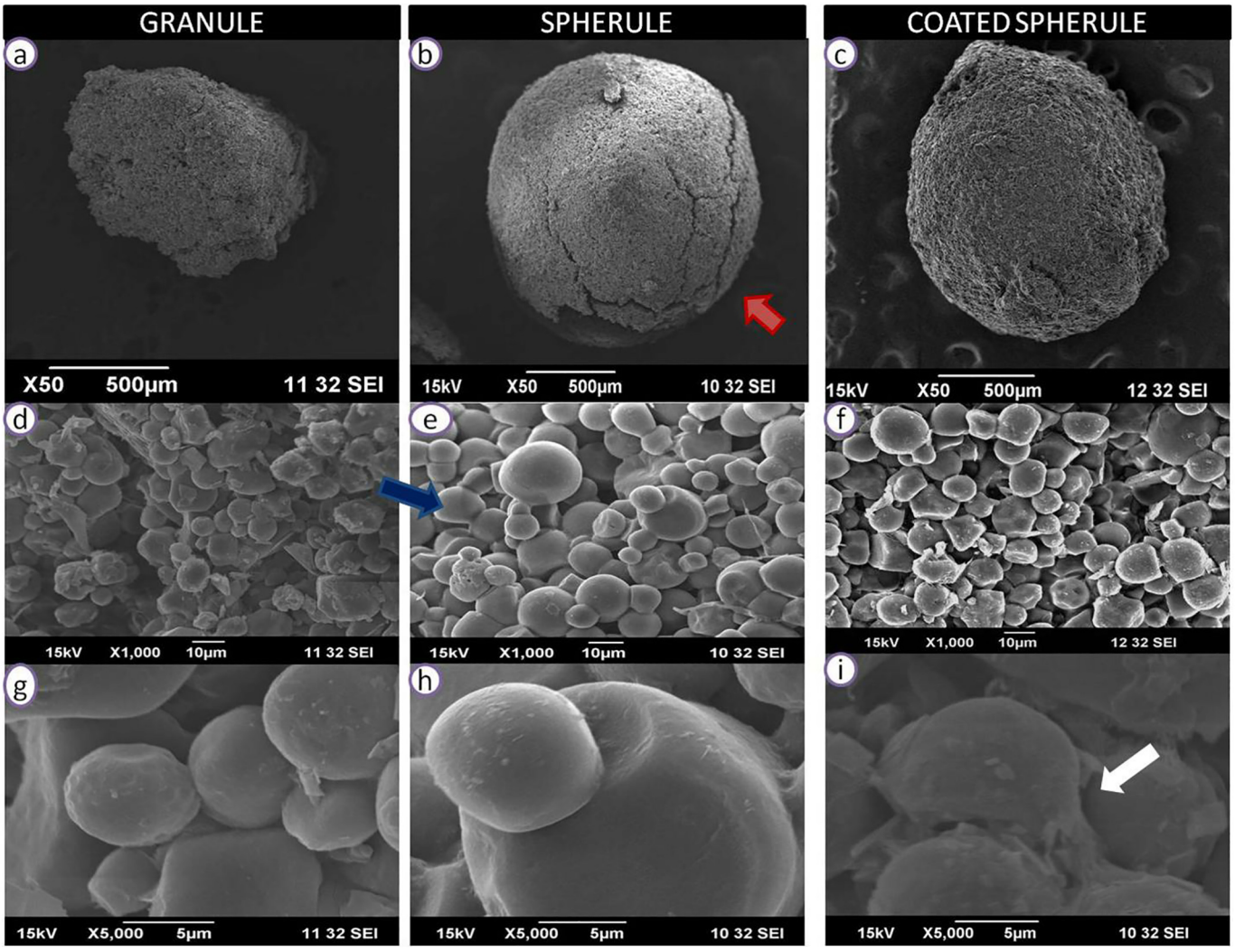

Fig. 6. Scanning electron microscopy of ASP granules, spherules, and EC coated spherules at different magnifications. Arrow, red (cracks), blue (Distributed packed particles), white (deposited polymeric material between the particles)

and the coating material is getting deposited mainly at the interstitial space of particles present at the surface of the spherules. The smaller particles present on the surface of granules, spherules, and coated spherules are starch particles. As the starch powder is used for the conversion of the granules to spherules. Given that, the drug content and drug release profile are studied as shown in Fig. 7, (here red and blue curves show drug release profiles for sieve no 22 (0.71 mm) and sieve no 44 (0.35 mm) respectively, for uncoated spherules (US-22/44); single coated EC and EL-100 spherules (S-EC-EG-C1-22/44); double-coated EC and EL-100 (S-EC-EG-C2-22/44); double-coated EC spherules (S-EC-C2-22/44)).

From Fig. 7, it shows that the uncoated spherules (f1) have a burst release of 80% whereas formulation f2 (single coated EC and EL-100 spherules) and f3 (double-coated EC and EL-100 spherules) show a slight decrease in the release (burst release 60%), which are not to the level of expectation, that may be because of an uncontrolled spray rate and a difference in rolling properties of spherules during the coating process [74] that affects the CE. But a beneficial control in the release is achieved by formulation f4 (double coated EC; burst release 40%).

Moreover, the coating on a bed of rolling particles can have several uncertainties, however, that can be optimized based on the threshold limit of controlling the release by the coated layer. Therefore the unseen uncertainties together can be accounted for within the concept of CE.

Here on a drug reservoir, the rate-controlled film coating is done [64]. The purpose of the study is to optimize the coating process. Experimentally, the coating process needs to be optimized to attain a relatively intact coating over the drug reservoir for control over the release rate. The coating process thus can be staged into a point that produces at least a 10% reduction in the release. Based on that the second coating may be decided that can produce an increase or decrease in the release. The increase in the release is due to increased osmotic pressure and enhanced diffusion. And the decrease can be due to the formation of intact less water diffusible membrane coating. These multiple coatings on a stage-by-stage manner can be considered together as CPC over the drug reservoir. This theory is evaluated in this work by taking four samples (f1, f2, f3 & f4). Where f1 is uncoated spherules (drug reservoir), f2 is a single coated spherule (drug reservoir with a partially coated surface and larger diffusible pores). For a single coated spherule (f2) a combination of EL-100 (hydrophilic polymer) [75] and EC (hydrophobic polymer) is used, f3 is a drug reservoir with an intact rate-controlling membrane having large hydrophilic pores. Here a second coating for the above coating is done once again (i.e. double coated EC and EL-100). And f4 is a drug reservoir with an intact hydrophobic rate-controlling membrane is prepared by doing with double coating using EC.

Further, mechanistic analysis of the drug release profile of spherules is done by fitting the drug release data to the various kinetic models (Table 7). Kinetic modeling of all the particles of spherules and coated spherules (uncoated and coated) retained in sieve no. 22 and 44 are analyzed, and that followed first-order drug release kinetics. All the spherules are showing $n < 0.45$ is an indication of the dissolution-based quasi-fickian release mechanism. This is mainly due to less water solubility of the drug molecule [65][76].

The f4 gives an intact coating around the drug reservoir with maximum demonstrated control over drug release, so this formulation is mainly analyzed for understanding the mechanism of release using various models. The regression analysis shows that the f4 follows 1st order release kinetics (Table 7). Where the regression coefficient for the f4 in 44 sieve (aperture size 0.35 mm) spherules is 0.99, hence it is following 1st order release kinetics as expected. Subsequently, the one that has

[i]

Spherules	Percentage Drug Content (%)
US-22	94.36±0.47
US-44	80.49±1.50
S-EC-EG-C1-22	81.28±0.31
S-EC-EG-C1-44	77.13±0.46
S-EC-EG-C2-22	85.9±0.92
S-EC-EG-C2-44	80.90±0.93
S-EC-C2-22	79.5± 0.77
S-EC-C2-44	73.5±1.27

[ii]

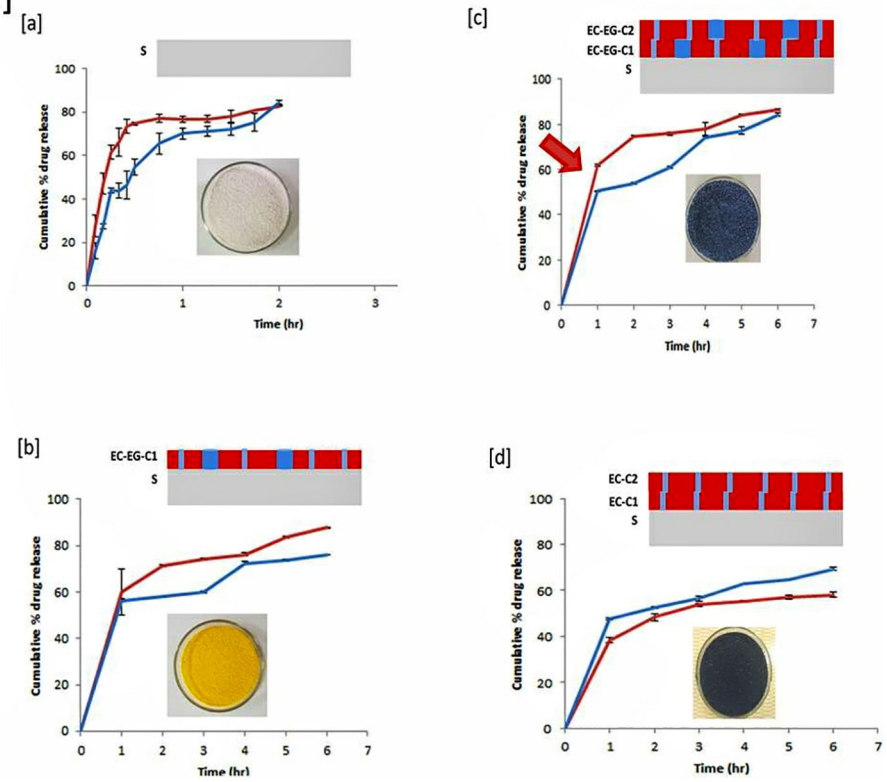

Fig. 7. Optimization of drug release of spherules, (i) Drug content evaluation of spherules. (ii) Drug release profile (red arrow indicates burst release) of, (a) Uncoated spherules (US-22/44), (b) Single coated with EC and Eudragit L-100 (S-EC-EG-C1-22/44) in 1:1 ratio. (c) Double coated with EC and Eudragit L-100 (S-EC-EG-C2-22/44).(d) Double coated with EC (S-EC-C2-22/44). Line graph of drug release for different spherules; (red) (Sieve No. 22), (blue) (Sieve No. 44),

Table 7
Mechanistic analysis of release kinetics of spherules retained in sieve numbers 22 and 44.

Kinetic models	Uncoated spherules (f1)			Single coated spherules (EC and Eudragit L-100 in 1:1 ratio) (f2)		Double coated EC and Eudragit L-100 spherules (f3)		Double coated EC spherules (f4)	
Sieve no.	22		44	22	44	22	44	22	44
Zero-order	R^2	0.70	0.48	0.66	0.66	0.62	0.80	0.66	0.69
	n	32.2	25.30	11.27	9.92	11.02	11.73	7.81	9.03
First-order	R^2	0.84	0.66	0.88	0.82	0.95	0.95	0.86	0.99
	n	0.32	0.28	0.13	0.08	0.08	0.10	0.03	0.04
Higuchi model	R^2	0.88	0.72	0.89	0.88	0.87	0.96	0.90	0.91
	n	56.68	48.71	33.68	29.45	33.47	32.96	23.4	26.6
Korsmeyer- Peppas model	R^2	0.60	0.88	0.96	0.83	0.95	0.91	0.94	0.96
	n	0.20	0.10	0.18	0.18	0.17	0.30	0.23	0.21

shown the highest regression coefficient (f4–44 sieve spherules) is taken as the point for the comparison of other samples.

The coated spherules are showing variation in n value depending upon the type and number of the coating. Between single coated and double coated EC/EL-100 spherules, the double-coated spherule is showing a higher n value. The increase in n value is an indication of enhanced release due to delivery system properties [77]. Usually, an increase in release happens due to the osmotic effect [78]. In such kinds of particles, the drug reservoir has osmotic properties due to the excipients [79]. From the n values, it is apparent that the osmotic pressure from the drug reservoir is more in the double coated than the single coated spherules. On the other hand, the hydrophobicity of the coated film is high in EC double-coated spherules; thus, the n value is further decreased, giving a higher control over release.

Given that, the DOS of optimized spherule is given in Fig. 4. The conversion of a granule to an f4 EC coated optimized spherule requires optimization of CPC and CE. The coating process is going through an arbitrary interface of less compact coating with varying release

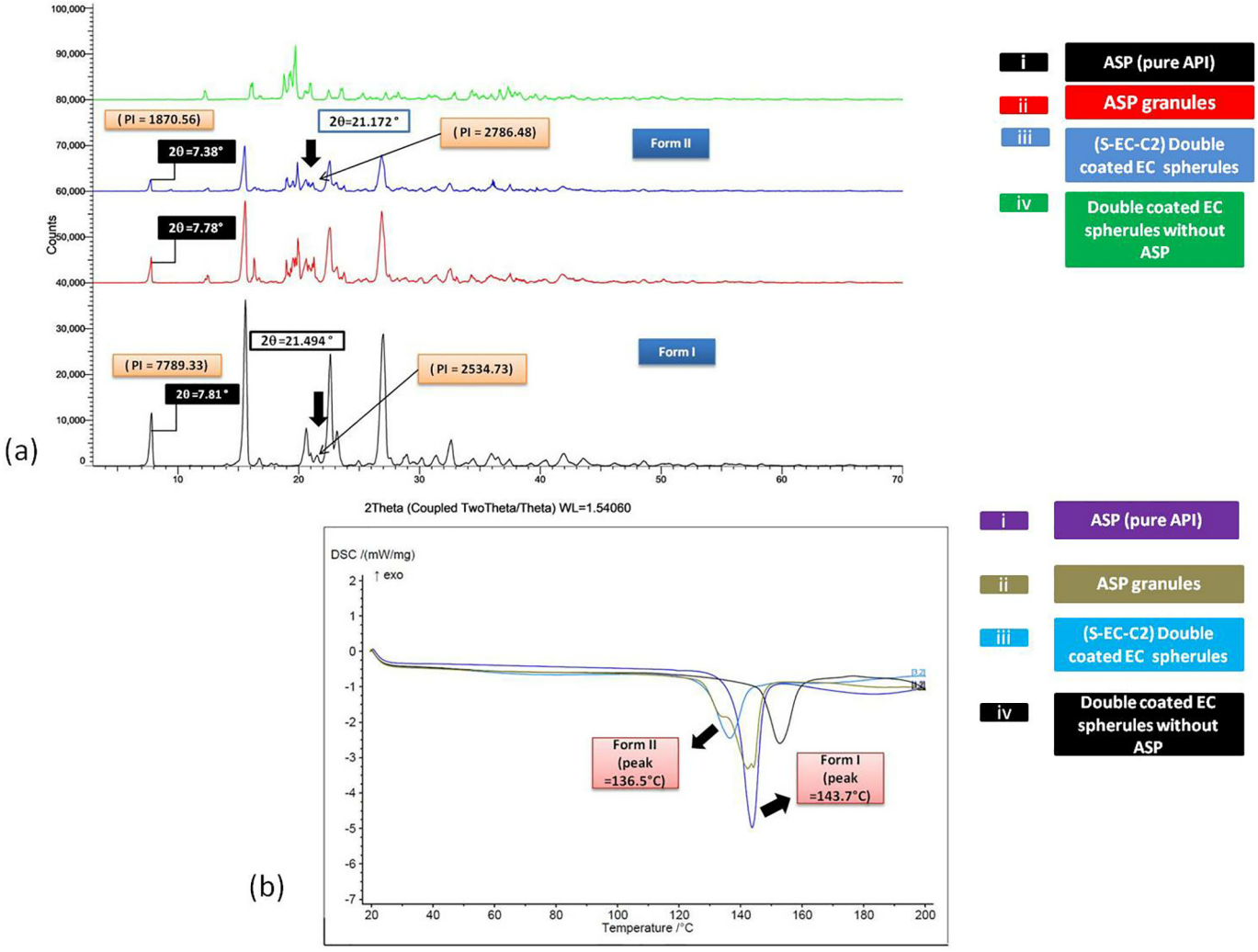

Fig. 8. PXRD and DSC analysis of prepared samples. (a) PXRD spectrum of (i) ASP (pure API), (ii) ASP granules, (iii) Double coated EC-ASP spherules (S-EC-C2), (iv) Double coated EC spherules without ASP. (b) DSC thermogram of (i) ASP (pure API), (ii) ASP granules, (iii) Double coated EC ASP spherules (S-EC-C2), (iv) Double coated EC spherules without ASP. Arrow (black) relevant peaks.

properties in the case of f2 (single coated EC and EL-100) and f3 (double coated EC and EL-100) respectively. While the f4 (EC double-coated spherule) being an intact coating is showing better control over the release. This is mainly due to enhanced hydrophobicity and intact coating achieved in the case of EC. To bring together the net outcome of the studies, EC coating on granules needs to be done on relatively larger particles, as multiple coatings, for maximum CPC and CE. The DOE predicts the required CPC for particular sustained-release properties. The experimental observation is fitting well with the DOE prediction (Table 6).

3.4. Powder X-ray diffraction (PXRD) and Differential scanning calorimetry (DSC) analysis

The PXRD data shows that (Fig. 8a), ASP remains in Form-I in the API with specific peaks intensity (PI) =2534.7, at 2θ =21.4^0 which is earlier confirmed as at 2θ =20.2^0 [80,81] and is maintained same in formulations as well. While double-coated EC spherules at 2θ = 21.172^0 (black arrow) indicating a Form-II polymorphic shift with peak intensity (PI) =2786.4. This shift needs to be further confirmed by DSC experiments.

The polymorphism of ASP from Form-I to Form-II is not clearly visible from XRD, even though its indications are there. However, the DSC experiments (Fig. 8b) indicate polymorphism that may be due to the introduction of the EC rate-controlling membrane. This is probably because of the partial solubilization of the ASP by the organic solvent (acetone) and its altered recrystallization in confinement due to the presence of a rate-controlling membrane. Here the organic solvent may be playing an important role in inducing the polymorphism. Because, in another process of preparation of granules by wet granulation in aqueous conditions, no endothermic peak shift in DSC from Form-I (143.7 °C) to Form-II (136.5 °C) is observed, while it remains at Form-I at peak =143.7 °C. That means organic solvent like acetone is causing polymorphism while the aqueous solvent is not.

The DSC data shows that (Fig. 8b) the ASP crystal structure is changing from Form-I with a melting point peak of 143.7 °C. Which was earlier identified as a peak at 143.9 °C [80], and is shifted to Form-II (136.5 °C) which is earlier identified as 135.5 °C [80] (Fig. 9).

This study shows a novel method to include arbitrary layers into the logic of DOE to analyze the role of independent variables on the responses (Figure 9:). . Here, the arbitrary layer adopted is CE, which is an intermediary stage before the required coating properties are achieved. By this method, the linear relation between the coating parameters and response such as release profile can be achieved. Also, a mechanistic understanding of the release properties with respect to coating parameters can be attained.

Further, the optimized EC-coated spherules can be blended with various other spherules (such as uncoated, single coated, and double-coated spherules) to achieve the desired release profile. They can have varying drug content and release properties. Moreover, this blending technique achieves tunable drug release patterns, suitable for enteric-coated, SR, and CR profiles [45]. These spherules are weighed and dosed before being filled into suitable hard gelatin capsules [74,82,83].

In this study, ASP granules are formulated into spherules. Spherules are produced by wet granulation followed by bed coating during rolling (BCDR) process. The novel BCDR technique is a robust and low-cost production technique used in the preparation of spherules for research and industrial applications.

These spherules have the therapeutic advantage such as high drug content, sustained release, and property of distribution over a wide area; being the spherules. That can result in improved absorption, decreased gastric irritation, which is particularly useful for treating the COVID-19 patients having sensitive mucosa [84]. Spherules are coated with sustained-release polymers that could avoid dissolution and disintegration of the dosage form in GIT while distributing the dose over a wide area of the intestine and deliver it over a period of time [41,85].

Although from various studies and published records [23,24], it is apparent that ASP possesses some antiviral properties. That also has a primary role in inhibiting the inflammatory responses and preventing cardiac dysfunction or myocardial infarction in COVID-19 patients. ASP is difficult to administer to COVID-19 patients, because of the inflammation, particularly in the stomach. Wherein, sustained-release formulations are most suited as demonstrated here. When compared to other NSAIDs like ibuprofen, administration of ASP at a low dose (i.e. less than 100 mg/day) is highly safe for long-term use [26].

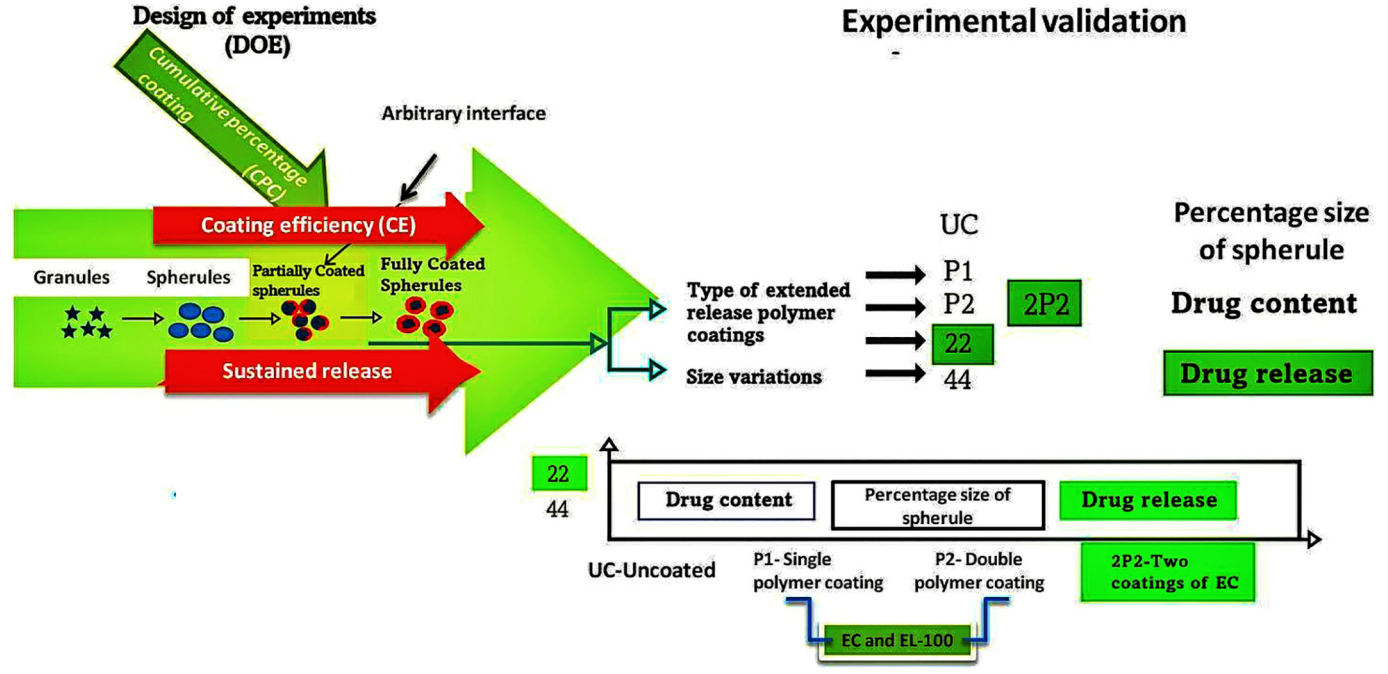

Fig. 9. Schematic representation of the study design and relation between the independent parameters such as CE, CPC, and responses (drug content, drug release, and percentage size of spherules) showing that CE and size affect the release from the spherules.(UC- Uncoated (f1), P1- single polymer coating (f2), P2- double polymer coating (f4)). Boxes (Green) (Optimised).

However, it causes side effects such as gastrointestinal bleeding or local toxicity due to the high concentration of drugs in the system [27]. The EC coated spherule-based technology rapidly developed here with the help of DOE is a suitable strategy to deliver ASP with minimal side effects in COVID-19 patients, as these spherules get distributed over a wide area and slowly deliver the ASP.

4. Conclusion

ASP is currently proposed as one of the candidate drugs for the treatment of COVID-19 patients due to its anticoagulant, anti-viral and anti-inflammatory properties. However, its local side effect during GI administration such as gastric irritation needs to be suppressed. This study aims to prepare an SR spherule-based oral formulation for ASP, from granules by modifying them using coating with an SR polymer (EC), to treat COVID-19. This is by optimizing the coating parameters and spherule properties by exploring DOE and experimental validation. For that, ASP spherules are developed using the novel BCDR process. They are then coated with EC sustained release polymer film coating and tested. The DOS by DOE is achieved to be around CE- 70.14%, CPC- 200% and DR- 61.54% as well as that is experimentally demonstrated. Comparison between DOE to experimentally validated results is shown within 20% deviation. The XRD and DSC analysis has demonstrated that ASP is undergoing polymorphism within the drug reservoir with respect to processing conditions, and this is the first report in this regard to our knowledge. The BCDR process and DOE with CE as an arbitrary interface are the novel techniques adopted here. This is for the quick optimization of SR formulations, which can be widely explored in the pharmaceutical industry. The optimization of EC coating based on mechanistic understanding of drug release profile adopted here also shed light on the design of SR coating requirements and optimization. One of the futuristic plans is to improve the stability of the ASP in spherules with respect to shelf-life.

The optimized spherules as demonstrated here are a potential candidate for the blending and filling of capsules to make as a unit dosage form.

Declaration of competing interest

The authors hereby declare that they don't have any conflict of interest on this manuscript.

Acknowledgement

We acknowledge the student research fund provided by Amrita Vishwa Vidyapeetham, AIMS Health Sciences Campus, Kochi, India. We also express our sincere gratitude to Dean Research, for the kind discussion and support and Principal, Amrita School of Pharmacy for all the support.

References

[1] T.M.S.U. Gunathilake, Y.C. Ching, C.H. Chuah, N.A. Rahman, N.S. Liou, Recent advances in celluloses and their hybrids for stimuli-responsive drug delivery, Int. J. Biol. Macromol. 158 (2020) 670–688, https://doi.org/10.1016/j.ijbiomac.2020.05.010.

[2] K.V. Vyshma, M. Hansan, M. Krishnapriya, P.P. Gayathri, E.U. Nithin, K. Juna, N. Antony, R. Renju, K. Kamalasanan, Formulation of different polymer-coated spherules from granules, 11 (4) (2019) 1633–1637.

[3] I. Elsayed, R.M. El-Dahmy, S.Z. El-Emam, A.H. Elshafeey, N.A.A. El Gawad, O.N. El-Gazayerly, Response surface optimization of biocompatible elastic nanovesicles loaded with rosuvastatin calcium: enhanced bioavailability and anticancer efficacy, Drug Deliv. Transl. Res. 10 (2020) 1459–1475, https://doi.org/10.1007/s13346-020-00761-0.

[4] S.K. Jain, M. Kaur, P. Kalyani, A. Mehra, N. Kaur, N. Panchal, Microsponges enriched gel for enhanced topical delivery of 5-fluorouracil, J. Microencapsul. 36 (2019) 677–691, https://doi.org/10.1080/02652048.2019.1667447.

[5] O.A. Adeleke, Premium ethylcellulose polymer based architectures at work in drug delivery, Int. J. Pharm. X. 1 (2019) 100023, https://doi.org/10.1016/j.ijpx.2019.100023.

[6] R. Macoon, T. Guerriero, A. Chauhan, Extended release of dexamethasone from oleogel based rods, J. Colloid Interface Sci. 555 (2019) 331–341, https://doi.org/10.1016/j.jcis.2019.07.082.

[7] C.K. Huang, K. Zhang, Q. Gong, D.G. Yu, J. Wang, X. Tan, H. Quan, Ethylcellulose-based drug nano depots fabricated using a modified triaxial electrospinning, Int. J. Biol. Macromol. 152 (2020) 68–76, https://doi.org/10.1016/j.ijbiomac.2020.02.239.

[8] T.H. Shin, M.J. Ho, S.R. Kim, S.H. Im, C.H. Kim, S. Lee, M.J. Kang, Y.W. Choi, Formulation and in vivo pharmacokinetic evaluation of ethyl cellulose-coated sustained release multiple-unit system of tacrolimus, Int. J. Biol. Macromol. 109 (2018) 544–550, https://doi.org/10.1016/j.ijbiomac.2017.12.111.

[9] L. Chen, G. Yang, X. Chu, C. Gao, Y. Wang, W. Gong, Z. Li, Y. Yang, M. Yang, C. Gao, Polymer distribution and mechanism conversion in multiple media of phase-separated controlled-release film-coating, Pharmaceutics. 11 (2019) 1–21, https://doi.org/10.3390/pharmaceutics11020080.

[10] B. Deeksha, V. Sadanand, N. Hariram, A.V. Rajulu, Preparation and properties of cellulose nanocomposite fabrics with in situ generated silver nanoparticles by bioreduction method, J. Bioresour. Bioprod. 6 (2021) 75–81, https://doi.org/10.1016/j.jobab.2021.01.003.

[11] D.W. Wei, H. Wei, A.C. Gauthier, J. Song, Y. Jin, H. Xiao, Superhydrophobic modification of cellulose and cotton textiles: methodologies and applications, J. Bioresour. Bioprod. 5 (2020) 1–15, https://doi.org/10.1016/j.jobab.2020.03.001.

[12] Z. Xia, J. Li, J. Zhang, X. Zhang, Processing and valorization of cellulose, lignin and lignocellulose using ionic liquids, J. Bioresour. Bioprod. 5 (2020) 79–95, https://doi.org/10.1016/j.jobab.2020.04.001.

[13] T. Yamada, H. Onishi, Y. Machida, Sustained release ketoprofen microparticles with ethylcellulose and carboxymethylethylcellulose, J. Control. Release 75 (2001) 271–282, https://doi.org/10.1016/S0168-3659(01)00399-6.

[14] Y. Fang, G. Wang, R. Zhang, Z. Liu, Z. Liu, X. Wu, D. Cao, Eudragit L/HPMCAS blend enteric-coated lansoprazole pellets: enhanced drug stability and oral bioavailability, AAPS PharmSciTech 15 (2014) 513–521, https://doi.org/10.1208/s12249-013-0035-1.

[15] S. Chen, F. Guo, T. Deng, S. Zhu, W. Liu, H. Zhong, H. Yu, R. Luo, Z. Deng, Eudragit S100-coated chitosan nanoparticles co-loading tat for enhanced oral colon absorption of insulin, AAPS PharmSciTech 18 (2017) 1277–1287, https://doi.org/10.1208/s12249-016-0594-z.

[16] C.L. Nemeth, W.R. Lykins, H. Tran, M.E.H. ElSayed, T.A. Desai, Bottom-up fabrication of multilayer enteric devices for the oral delivery of peptides, Pharm. Res. 36 (2019) https://doi.org/10.1007/s11095-019-2618-3.

[17] Q. Ruan, K. Yang, W. Wang, L. Jiang, J. Song, Clinical predictors of mortality due to COVID-19 based on an analysis of data of 150 patients from Wuhan, China, Intensive Care Med. 46 (2020) 846–848, https://doi.org/10.1007/s00134-020-05991-x.

[18] J.D. McFadyen, H. Stevens, K. Peter, The emerging threat of (micro)thrombosis in COVID-19 and its therapeutic implications, Circ. Res. 127 (2020) 571–587, https://doi.org/10.1161/CIRCRESAHA.120.317447.

[19] J. Petäjä, Inflammation and coagulation. An overview, Thromb. Res. 127 (2011) 34–37, https://doi.org/10.1016/S0049-3848(10)70153-5.

[20] K. Kamalasanan, Biomimetic conjoining pathways for COVID-19 nanomedicine drug discovery and medical devices: prophylactic medicines as alternative for vaccines, Trends Biomater. Artif. Organs 34 (2020) 8–11.

[21] S. Salim, K. Kamalasanan, Controlled drug delivery for alopecia: a review, J. Control. Release 325 (2020) 84–99, https://doi.org/10.1016/j.jconrel.2020.06.019.

[22] S.V. Ittaman, J.J. VanWormer, S.H. Rezkalla, The role of aspirin in the prevention of cardiovascular disease, Clin. Med. Res. 12 (2014) 147–154, https://doi.org/10.3121/cmr.2013.1197.

[23] NCT04365309, Protective effect of aspirin on COVID-19 patients, Https://Clinicaltrials.Gov/Show/NCT04365309 2020https://www.cochranelibrary.com/central/doi/10.1002/central/CN-02103526/full.

[24] B. Glatthaar-Saalmüller, K.H. Mair, A. Saalmüller, Antiviral activity of aspirin against RNA viruses of the respiratory tract—an in vitro study, Influenza Other Respir. Viruses 11 (2017) 85–92, https://doi.org/10.1111/irv.12421.

[25] Y. Dai, J. Ge, Clinical use of aspirin in treatment and prevention of cardiovascular disease, Thrombosis. 2012 (2012) 1–7, https://doi.org/10.1155/2012/245037.

[26] P.F. Haastrup, T. Grønlykke, D.E. Jarbøl, Enteric coating can lead to reduced antiplatelet effect of low-dose acetylsalicylic acid, Basic Clin. Pharmacol. Toxicol. 116 (2015) 212–215, https://doi.org/10.1111/bcpt.12362.

[27] C. J. Lavie, C. W. Howden, J. Scheiman, J. Tursi. Upper gastrointestinal toxicity associated with long-term aspirin therapy: consequences and prevention. CurrProbICardiol. 2017 May;42(5):146–164. doi: https://doi.org/10.1016/j.cpcardiol.2017.01.006. Epub2017 Feb 1. PMID: 28363584.

[28] K.P. Bliden, J. Patrick, A.T. Pennell, U.S. Tantry, P.A. Gurbel, Drug delivery and therapeutic impact of extended-release acetylsalicylic acid, FutureCardiol. 12 (1) (2016 Jan) 45–58, https://doi.org/10.2217/fca.15.60 , Epub 2015 Sep 10 26356085.

[29] C. Maderuelo, J.M. Lanao, A. Zarzuelo, Enteric coating of oral solid dosage forms as a tool to improve drug bioavailability, Eur. J. Pharm. Sci. 138 (2019) 105019, https://doi.org/10.1016/j.ejps.2019.105019.

[30] Y. Chen, Z.N. Liu, B. Li, T. Jiang, Preparation of aspirin sustained-release microsphere and its in vitro releasing property, Beijing da xuexuebao, Yi xue ban = Journal of Peking University. Health Sciences 51 (5) (2019 Oct) 907–912, https://doi.org/10.19723/j.issn.1671-167x.2019.05.019.

[31] J. Patrick, A. Johnson, L. Dillaha, A.T. Pennell, Safety and tolerability of extended-release acetylsalicylic acid capsules: a summary of double-blind comparative studies, Futur. Cardiol. 12 (2016) 627–638, https://doi.org/10.2217/fca-2016-0042.

[32] A. Touzet, F. Pfefferlé, A. Lamprecht, Y. Pellequer, Formulation of ketoconazole nanocrystal-based cryopellets, AAPS PharmSciTech 21 (2) (2020 Jan 3) 50, https://doi.org/10.1208/s12249-019-1570-131900727.

[33] M. Wang, J. Hou, D.G. Yu, S. Li, J. Zhu, Z. Chen, Electrospun tri-layer nanodepots for sustained release of acyclovir, J. Alloys Compd. 846 (2020) 156471, https://doi.org/10.1016/j.jallcom.2020.156471.
[34] Y. Yang, S. Chang, Y. Bai, Y. Du, D.G. Yu, Electrospun triaxial nanofibers with middle blank cellulose acetate layers for accurate dual-stage drug release, Carbohydr. Polym. 243 (2020) 116477, https://doi.org/10.1016/j.carbpol.2020.116477.
[35] K. Wang, P. Wang, M. Wang, D.G. Yu, F. Wan, S.W.A. Bligh, Comparative study of electrospun crystal-based and composite-based drug nano depots, Mater. Sci. Eng. C 113 (2020) 110988, https://doi.org/10.1016/j.msec.2020.110988.
[36] K.I. Al-Malah, Optimization of drug solubility using aspen plus: acetylsalicylic acid (aspirin) solubility – a second case study, Asian J. Pharm. Clin. Res. 13 (2020) 178–184, https://doi.org/10.22159/ajpcr.2020.v13i4.37143.
[37] B. Miller, R. Mirakian, S. Gane, J. Larco, A.A. Sannah, Y. Darby, G. Scadding, Nasal lysine aspirin challenge in the diagnosis of aspirin - exacerbated respiratory disease, Exp. Allergy (2013) 874–880, https://doi.org/10.1111/cea.12110.
[38] M. Roberts, M. Cespi, J.L. Ford, A.M. Dyas, J. Downing, L.G. Martini, P.J. Crowley, Influence of ethanol on aspirin release from hypromellose matrices, Int. J. Pharm. 332 (2007) 31–37, https://doi.org/10.1016/j.ijpharm.2006.09.055.
[39] L. L. Chang, M. J. Pikal. Mechanisms of protein stabilization in the solid state. J Pharm Sci. 2009 Sep;98(9):2886–908. doi: https://doi.org/10.1002/jps.21825. PMID: 19569054.
[40] M. Korang-Yeboah, Z. Rahman, D. Shah, A. Mohammad, S. Wu, A. Siddiqui, M.A. Khan, Impact of formulation and process variables on solid-state stability of theophylline in controlled release formulations, Int. J. Pharm. 499 (1–2) (2016 Feb 29) 20–28, https://doi.org/10.1016/j.ijpharm.2015.11.046 , Epub 2015 Dec 11 26688036.
[41] M. Choi, S.C. Porter, B. Macht, A. Meisen, Novel coating uniformity models for tablet pan coaters, AAPS PharmSciTech. 22, 2021https://doi.org/10.1208/s12249-020-01857-z.
[42] N. Shah, T. Mehta, R. Aware, V. Shetty, Investigation on influence of Wurster coating process parameters for the development of delayed release minitablets of Naproxen, Drug Dev. Ind. Pharm. 43 (2017) 1989–1998, https://doi.org/10.1080/03639045.2017.1357732.
[43] U. Kestur, D. Desai, Z. Zong, A. Abraham, J. Fiske, Effect of coating excipients on chemical stability of active coated tablets, Pharm. Dev. Technol. 26 (2021) 41–47, https://doi.org/10.1080/10837450.2020.1832520.
[44] P. Böhling, J.G. Khinast, D. Jajcevic, C. Davies, A. Carmody, P. Doshi, M.T. AmEnde, A. Sarkar, Computational fluid dynamics-discrete element method modeling of an industrial-scale WursterCoater, J. Pharm. Sci. 108 (1) (2019 Jan) 538–550, https://doi.org/10.1016/j.xphs.2018.10.016 , Epub 2018 Oct 16 30339868.
[45] Y. Yang, H. Wang, H. Li, Z. Ou, G. Yang, 3D Printed Tablets with Internal Scaffold Structure Using Ethyl Cellulose to Achieve Sustained Ibuprofen Release, Elsevier B. V 2018https://doi.org/10.1016/j.ejps.2018.01.005.
[46] X. Shen, D. Yu, L. Zhu, C. Branford-White, K. White, N.P. Chatterton, Electrospun diclofenac sodium loaded Eudragit® L 100-55 nanofibers for colon-targeted drug delivery, Int. J. Pharm. 408 (2011) 200–207, https://doi.org/10.1016/j.ijpharm.2011.01.058.
[47] J.H. Wu, X.J. Wang, S.J. Li, X.Y. Ying, J.B. Hu, X.L. Xu, X.Q. Kang, J. You, Y.Z. Du, Preparation of ethyl cellulose microspheres for sustained release of sodium bicarbonate, Iran. J. Pharm. Res. 18 (2) (2019) 556–568, https://doi.org/10.22037/ijpr.2019.1100651 Spring. PMID: 31531041; PMCID: PMC6706755.
[48] A.K. Bani-Jaber, M.Y. Alkawareek, J.J. Al-Gousous, A.Y. Abu Helwa, Floating and sustained-release characteristics of effervescent tablets prepared with a mixed matrix of eudragit L-100-55 and eudragit E PO, Chem. Pharm. Bull. 59 (2011) 155–160, https://doi.org/10.1248/cpb.59.155.
[49] F. Sadeghi, J.L. Ford, M.H. Rubinstein, A.R. Rajabi-Siahboomi, Comparative study of drug release from pellets coated with HPMC or Surelease, Drug Dev. Ind. Pharm. 26 (6) (2000 Jun) 651–660, https://doi.org/10.1081/ddc-10010128010826113.
[50] L.A. Felton, S.C. Porter, An update on pharmaceutical film coating for drug delivery, Expert Opin. Drug Deliv. 10 (4) (2013 Apr) 421–435, https://doi.org/10.1517/17425247.2013.763792 , Epub 2013 Jan 23 23339342.
[51] B. Singh, S.K. Chakkal, N. Ahuja, Formulation and optimization of controlled release mucoadhesive tablets of atenolol using response surface methodology, AAPS PharmSciTech 7 (2006) 1–10, https://doi.org/10.1208/pt070103.
[52] A. Mujtaba, M. Ali, K. Kohli, Formulation of extended release cefpodoxime proxetil chitosan-alginate beads using quality by design approach, Int. J. Biol. Macromol. 69 (2014) 420–429, https://doi.org/10.1016/j.ijbiomac.2014.05.066.
[53] D. Soans, R. Chandramouli, A.N. Kavitha, S.K. Roopesh, S. Shrestha, Application of design of experiments for optimizing critical quality attributes (CQA) in routine pharmaceutical product development, J. Pharm. Res. 15 (2016) 96, https://doi.org/10.18579/jpcrkc/2016/15/3/103041.
[54] F. and D. Administration, Guidance for Industry, PAT-A Framework for Innovative Pharmaceutical Development, Manufacturing and Quality Assurance, http://www.fda.gov/downloads/Drugs/GuidanceComplianceRegulatoryInformation/Guidances/ucm070305.pdf 2004.
[55] R. Calfee, D. Piontkowski, Design and analysis of experiments, Handb. Read. Res. (2016) 63–90, https://doi.org/10.2307/2983009.
[56] P. Vishweshwar, J.A. McMahon, M. Oliveira, M.L. Peterson, M.J. Zaworotko, The predictably elusive form II of aspirin, J. Am. Chem. Soc. 127 (2005) 16802–16803, https://doi.org/10.1021/ja056455b.
[57] S.K. Flores, D. Costa, F. Yamashita, L.N. Gerschenson, M. VGrossmann, Mixture design for evaluation of potassium sorbate and xanthan gum effect on properties of tapioca starch films obtained by extrusion, Mater. Sci. Eng. C 30 (1) (2010) 196–202, https://doi.org/10.1016/j.msec.2009.10.001.
[58] V.I. Bobkov, V.V. Borisov, M.I. Dli, V.P. Meshalkin, Modeling the calcination of phosphorite pellets in a dense bed, Theor. Found. Chem. Eng. 49 (2015) 176–182, https://doi.org/10.1134/S0040579515020025.
[59] R.B. Shah, M.A. Tawakkul, M.A. Khan, Comparative evaluation of flow for pharmaceutical powders and granules, AAPS PharmSciTech 9 (2008) 250–258, https://doi.org/10.1208/s12249-008-9046-8.
[60] D.P. Sinica, S.G. Sudke, D.M. Sakarkar, Application of hot-melt coating for sustained release pellets of fenoverine, Der Pharm. Sin. 4 (2013) 153–159.
[61] F.A.E. Mahmoud, K.S. Hashem, A.M.M. Hussein Elkelawy, The effect of aspirin nanoemulsion on TNFα and iNOS in gastric tissue in comparison with conventional aspirin, Int. J. Nanomedicine 10 (2015) 5301–5308, https://doi.org/10.2147/IJN.S86947.
[62] S. Fukui, H. Yano, S. Yada, T. Mikkaichi, H. Minami, Design and evaluation of an extended-release matrix tablet formulation; the combination of hypromellose acetate succinate and hydroxypropylcellulose, Asian J. Pharm. Sci. 12 (2017) 149–156, https://doi.org/10.1016/j.ajps.2016.11.002.
[63] D.J. Phillips, S.R. Pygall, V.B. Cooper, J.C. Mann, Overcoming sink limitations in dissolution testing: a review of traditional methods and the potential utility of biphasic systems, J. Pharm. Pharmacol. 64 (2012) 1549–1559, https://doi.org/10.1111/j.2042-7158.2012.01523.x.
[64] V. Dash, S.K. Mishra, M. Singh, A.K. Goyal, G. Rath, Release kinetic studies of aspirin microcapsules from ethyl cellulose, cellulose acetate phthalate and their mixtures by emulsion solvent evaporation method, Sci. Pharm. 78 (2010) 93–101, https://doi.org/10.3797/scipharm.0908-09.
[65] R.A. Bataglioli, J.B.M. Rocha Neto, B.S. Leão, L.G.L. Germiniani, T.B. Taketa, M.M. Beppu, Interplay of the assembly conditions on drug transport mechanisms in polyelectrolyte multilayer films, Langmuir 36 (42) (2020 Oct 27) 12532–12544, https://doi.org/10.1021/acs.langmuir.0c01980 Epub 2020 Oct 16. PMID: 33064494; PMCID: PMC7660939.
[66] L. Murray, H. Nguyen, Y. Lee, M.D. Remmenga, D.W. Smith, New Prairie Press Variance Inflation Factors in Regression Models With, Conf. Appl. Stat, Agric, 2012https://doi.org/10.4148/2475-7772.1034.
[67] B. Singh, R. Bhatowa, C.B. Tripathi, R. Kapil, Developing micro-/nanoparticulate drug delivery systems using “design of experiments”, Int. J. Pharm. Investig. 1 (2011) 75–87, https://doi.org/10.4103/2230-973X.82395.
[68] M. Cavinato, E. Andreato, M. Bresciani, I. Pignatone, G. Bellazzi, E. Franceschinis, N. Realdon, P. Canu, A.C. Santomaso, Combining formulation and process aspects for optimizing the high-shear wet granulation of common drugs, Int. J. Pharm. 416 (2011) 229–241, https://doi.org/10.1016/j.ijpharm.2011.06.051.
[69] V. De Simone, A. Dalmoro, G. Lamberti, D. Caccavo, M. d'Amore, A.A. Barba, HPMC granules by wet granulation process: effect of vitamin load on physicochemical, mechanical and release properties, Carbohydr. Polym. 181 (2018) 939–947, https://doi.org/10.1016/j.carbpol.2017.11.056.
[70] E. Mwesigwa, A.W. Basit, An investigation into moisture barrier film coating efficacy and its relevance to drug stability in solid dosage forms, Int. J. Pharm. 497 (2016) 70–77, https://doi.org/10.1016/j.ijpharm.2015.10.068.
[71] A.P. Sergio, S. FIsabelde, B.M. José, F.J. Otero-Espinar, Fast and controlled release of triamcinolone acetonide from extrusion-spheronization pellets based on mixtures of native starch with dextrin or waxy maize starch, Drug Dev. Ind. Pharm. 33 (9) (2007 Sep) 945–951, https://doi.org/10.1080/03639040601128720178915 80.
[72] N. Shah, T. Mehta, M. Gohel, Formulation and optimization of multiparticulate drug delivery system approach for high drug loading, AAPS PharmSciTech 18 (2017) 2157–2167, https://doi.org/10.1208/s12249-016-0689-6.
[73] M.N.U. Nguyen, P.H.L. Tran, T.T.D. Tran, A single-layer film coating for colon-targeted oral delivery, Int. J. Pharm. 559 (2019) 402–409, https://doi.org/10.1016/j.ijpharm.2019.01.066.
[74] S.C. Basak, K. Kaladhar, Doxycycline hyclate delayed release capsules with sodium starch glycolate as a pH- dependent pore forming agent, *Indian J. Pharm*. Sci. 66 (2004) 704–707.
[75] I. Speer, V. Lenhart, M. Preis, J. Breitkreutz, Prolonged release from orodispersible films by incorporation of diclofenac-loaded micropellets, Int. J. Pharm. 554 (2019) 149–160, https://doi.org/10.1016/j.ijpharm.2018.11.013.
[76] A. Olejnik, A. Kapuscinska, G. Schroeder, I. Nowak, Physico-chemical characterization of formulations containing endomorphin-2 derivatives, Amino Acids 49 (2017) 1719–1731, https://doi.org/10.1007/s00726-017-2470-x.
[77] E. Karavas, E. Georgarakis, D. Bikiaris, Application of PVP/HPMC miscible blends with enhanced mucoadhesive properties for adjusting drug release in predictable pulsatile chronotherapeutics, Eur. J. Pharm. Biopharm. 64 (1) (2006 Aug) 115–126, https://doi.org/10.1016/j.ejpb.2005.12.013 , Epub 2006 May 3 16675210.
[78] S. Jeong, S. Jeong, S. Chung, A. Kim, Revisiting in vitro release test for topical gel formulations: the effect of osmotic pressure explored for better biorelevance, Eur. J. Pharm. Sci. 112 (2018) 102–111, https://doi.org/10.1016/j.ejps.2017.11.009.
[79] G. Jiang, B.C. Thanoo, P.P. DeLuca, Effect of osmotic pressure in the solvent extraction phase on BSA release profile from PLGA microspheres, Pharm. Dev. Technol. 7 (2002) 391–399, https://doi.org/10.1081/PDT-120015040.
[80] P.P. Bag, C.M. Reddy, Screening and selective preparation of polymorphs by fast evaporation method: a case study of aspirin, anthranilic acid, and niflumic acid, Cryst. Growth Des. 12 (2012) 2740–2743, https://doi.org/10.1021/cg300404r.
[81] C. Ouvrard, S.L. Price, Toward crystal structure prediction for conformationally flexible molecules: the headaches illustrated by aspirin, Cryst. Growth Des. 4 (2004) 1119–1127, https://doi.org/10.1021/cg049922u.

[82] S.C. Basak, K. Kaladhar, T. Subburaj, Studies in formulation of delayed release capsules of doxycycline hyclate, ACTA PharmaceuticaSciencia 48 (2) (2006) 121–128.

[83] M.A. Sallam, M.T.M. Boscá, Optimization, ex vivo permeation, and stability study of lipid nanocarrier loaded gelatin capsules for treatment of intermittent claudication, Int. J. Nanomedicine 10 (2015) 4459–4478, https://doi.org/10.2147/IJN.S83123.

[84] B. Cryer, K.W. Mahaffey, Gastrointestinal ulcers, role of aspirin, and clinical outcomes: pathobiology, diagnosis, and treatment, J. Multidiscip. Healthc. 7 (2014) 137–146, https://doi.org/10.2147/JMDH.S54324.

[85] Y. Huang, Z. Huang, M. Wu, Y. Liu, C. Ma, X. Zhang, Z. Zhao, X. Bai, H. Liu, L. Wang, X. Pan, C. Wu, Modified-release oral pellets for duodenum delivery of doxycycline hyclate, Drug Dev. Res. 80 (2019) 958–969, https://doi.org/10.1002/ddr.21575.